ELSEVIER

Thermochimica Acta 244 (1994) 223–234

thermochimica acta

Cationic distribution and mechanism of the oxidation of V^{3+} ions in vanadium-substituted magnetites

M. Nohair, P. Perriat, B. Domenichini, B. Gillot *

Laboratoire de Recherche sur la Réactivité des Solides associé au CNRS, URA 23, Faculté des Sciences Mirande, B.P. 138, 21004 Dijon Cedex, France

Received 13 August 1993; accepted 13 February 1994

Abstract

The thermal behavior in oxygen of $Fe_{3-x}V_xO_4$ spinels ($0 < x < 1$) prepared by the ceramic method has been investigated over the temperature range 150–650°C by thermogravimetry and infrared spectroscopy. Below 500°C, iron vanadium spinels are partly oxidized in cation-deficient spinels with a large content of vacancies. A quantitative analysis based on the difference in the reactivity of iron and vanadium in relation to the site occupied (octahedral B site or tetrahedral A site) permits a cation distribution between the sub-lattices to be proposed. Kinetic studies of the oxidation process of V^{3+} ions at the B sites show that the oxidation reaction is controlled by cation diffusion in a cation-deficient spinel phase of variable composition, with a chemical diffusion coefficient dependent on the vacancy content δ and written: $\tilde{D} = K_0 \exp(-E_a/RT) \exp(-b\delta)$. The b constant depends on the temperature. The energy of defect dissociation has been determined.

Keywords: Cation; DTG; FTIR; Magnetite; Oxidation; Spinel; Vanadium compound; XRD

1. Introduction

The cation distribution and the valence state of vanadium in transition metal oxides of formulae $Fe_{3-x}V_xO_4$ ($0 < x < 2$) have been investigated by several workers employing various measurement techniques [1–11]. However, there has been little agreement on the distribution of iron and vanadium ions among the

* Corresponding author.

SSDI 0040-6031(94)01767-B

octahedral (B) and tetrahedral (A) sites of the spinel structure. For example, in the spinel Fe_2VO_4, the cation distribution has been variously to assume to be

$$(Fe^{2+})_A(Fe^{2+}V^{4+})_BO_4^{2-} \quad [1,2] \tag{1}$$

$$(Fe^{3+})_A(Fe^{2+}V^{3+})_BO_4^{2-} \quad [5,6,11] \tag{2}$$

$$(Fe^{2+}_{1-\lambda}Fe^{3+}_{\lambda})_A(Fe^{2+}_{\lambda}Fe^{3+}_{1-\lambda}V^{3+})_BO_4^{2-} \tag{3}$$

with $\lambda = 0$ [3], $\lambda = 1$ [4–6] and $0 < \lambda < 1$ [7,9].

For the range of solid solutions from Fe_3O_4 to Fe_2VO_4, the cation distribution

$$(Fe^{3+})_A(Fe^{2+}Fe^{3+}_{x-1}V^{3+}_{2-x})_BO_4^{2-} \tag{4}$$

has been suggested [5]; this is consistent with the observation of Fe^{3+} and V^{3+} ions coexisting on equivalent B sites and with the high electrical conductivity resulting from electronic exchange between the Fe^{2+} and Fe^{3+} ions on these sites [9]. The good electrical conductivity in a spinel associated with a mixed cation valence on energetically equivalent neighbouring lattice sites makes it possible to eliminate distributions (1) and (2). Although transport properties and Mössbauer measurements [8] support distribution (4), the data are also consistent with the valency distribution

$$(Fe^{3+}_{1-0.5x}Fe^{2+}_{0.5x})_A(Fe^{2.5+}_{2-x}V^{3+}_{x})_BO_4^{2-} \tag{5}$$

when the introduction of trivalent solutes has been seen to introduce a transfer of Fe^{2+} ions from B to A sites. Moreover, the possibility of a mixed V^{2+}/V^{3+} valence coinciding with a mixed Fe^{2+}/Fe^{3+} valence must also be entertained, as the energy difference between the two couples appears to be small [10]. For $x = 1$, a 10% V^{2+} concentration is consistent with the observed paramagnetic Curie constant [11]. A mean valence of $Fe^{2.5+}$ indicates that the Fermi energy of the stable spinel intersects three overlapping redox couples: the Fe^{3+}/Fe^{2+} couple at both the A and B sites, and the V^{3+}/V^{2+} couple at the B sites.

This paper reports the results of such a study by quantitative analysis from derivative thermogravimetry (DTG). This analysis is based on the discrepancy of reactivity between oxidizable cations located at both the A and B sites of the spinel structure [12] when it has been previously established that the oxidation temperature at B-site M^{n+} ions is lower than that at A-site M^{n+} ions. Moreover, the possible occupation of B sites by several oxidizable cations (Fe^{2+}, V^{2+}, V^{3+}) requires a careful consideration of the relative availability for oxidation of these different cations located in the same sub-lattice. Because it is possible for each cation in a spinel structure to be oxidized separately [13], the oxidation kinetics of vanadium ions has also been performed. The interest in this study lies in the possibility of testing the influence of vacancy content on the chemical diffusion coefficient when the oxidation leads to the formation of cation-deficient spinels.

2. Experimental procedure

The iron–vanadium oxides, $Fe_{3-x}V_xO_4$, were prepared by mixing in an agate mortar powders of Fe, Fe_2O_3 and V_2O_3 of spectroscopic grade in adequate molar

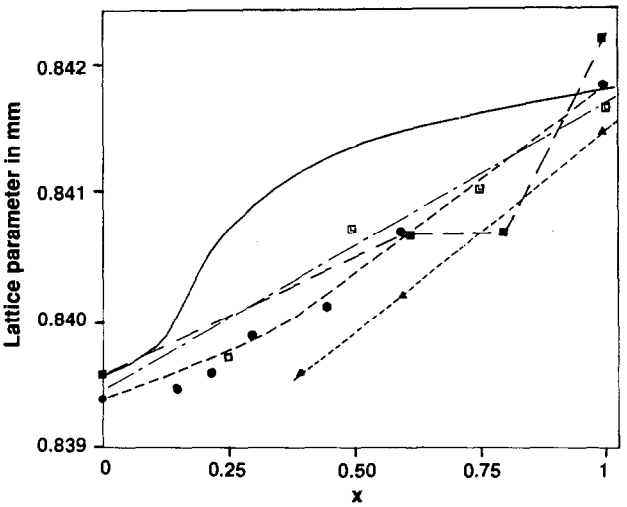

Fig. 1. Compositional dependence of lattice parameter for spinels $Fe_{3-x}V_xO_4$: □, this work; ●, from ref. 5; ▲, from ref. 14; ■, from ref. 15; ——, calculated from the Poix method with cation distribution (6).

ratios with various values of x ($0 < x < 1$). The well-homogenized powder was put inside a silica ampoule. This was then degassed under vacuum in order to avoid oxidation at high temperature, sealed, heated at 850°C for 24 h, and finally the samples were left to cool down in the furnace at a rate of about 5 K min^{-1}. All the samples were shown to be single-phase spinel and stoichiometric by X-ray diffractometry and thermogravimetric analysis, respectively. The lattice parameter increased from 0.8396 nm ($x = 0$) to 0.8417 nm ($x = 1$). If we compare our results to previous investigations, the values are in good agreement with earlier values reported in refs. 5, 14 and 15 (Fig. 1).

The samples were also characterized by infrared spectroscopy. In the region investigated (1100–100 cm^{-1}), the spectra reveal two strong absorption bands (Fig. 2) ν_1 and ν_2 which, for $x = 0.10$, occur at 570 and 370 cm^{-1}, and for $x = 1$, at 575 and 425 cm^{-1}. The position of the band ν_2 which is an M–O stretching mode of the octahedral sites [16] changes strongly with x, due to the variation in the Fe^{3+}–O^{2-} complexes with increasing vanadium content. In addition to the Fe^{3+} ions at the B sites, V^{3+} ions are also present [11]. With an increase in the V^{3+}–O^{2-} octahedral complexes, an increase in the intensity of the shoulder at about 420 cm^{-1} is expected [17,18]. This implies that with the increase in the V^{3+}–O^{2-} complexes, the band at 370 cm^{-1} should disappear at higher vanadium content, indicating a stronger ionic bonding for V^{3+}–O^{2-} complexes.

The average particle size of these loose powders measured from enlarged SEM images was only 0.3 μm, which is due to the low preparation temperature; this allows their oxidation to cation-deficient spinels [19]. After a prolonged strong grinding, the grain size was maintained but the samples were slightly oxidized during the grinding.

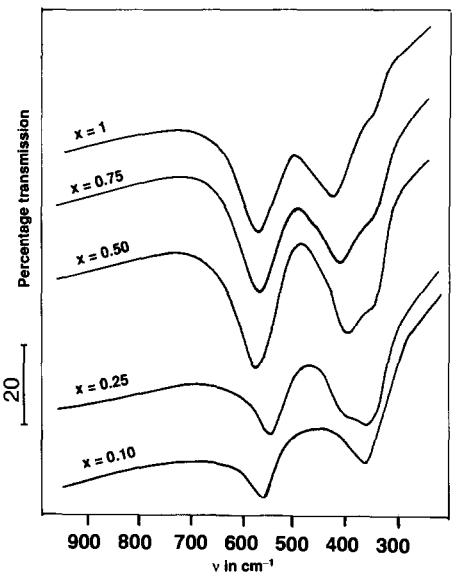

Fig. 2. IR spectra of initial samples.

The oxidations were performed under isothermal conditions or with the temperature increasing at a linear rate (2.5°C min^{-1}) in a Setaram MTB 10-8 microbalance using 6 mg of powder. The oxidation degree of the samples at various levels of reaction was calculated from the gravimetric data.

The IR spectra were recorded with a Perkin-Elmer 1725X FTIR spectrometer over the range 4000–400 cm^{-1} and with a Perkin-Elmer 1700 FTIR spectrometer over the range 500–50 cm^{-1}. About 1 mg of sample was mixed with 200 mg of spectroscopically pure dry CsI or with 50 mg of polyethylene and pressed into disks before recording the spectra.

3. Results and discussion

3.1. Cationic distribution

The determination of the cationic distribution was performed directly using derivative thermogravimetry. As a matter of fact, previous studies have demonstrated that if a compound oxidizes in cation-deficient spinel, DTG curves can be used to separate the oxidation peaks of the different oxidizable cations, the area of each peak being indicative of the quantities of each oxidizable cation within the spinel [20]. As the samples can be partly oxidized in cation-deficient spinels under various expeirmental conditions, the DTG technique can be employed.

When the samples are heated in air at a constant rate (Fig. 3), two regions corresponding to distinct oxidation reactions can be distinguished. In the first

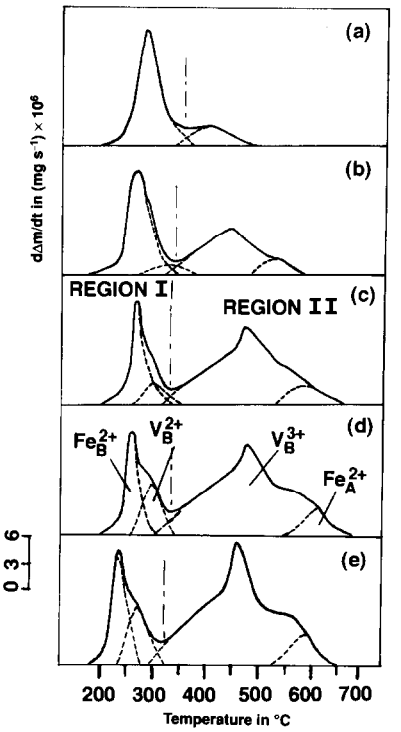

Fig. 3. DTG curves $d\Delta m/dt = f(T)$ (——) and deconvolution of curves (– – –) for $Fe_{3-x}V_xO_4$ ferrites versus vanadium content: (a) $x = 0.10$; (b) $x = 0.25$; (c) $x = 0.50$; (d) $x = 0.75$; (e) $x = 1$.

region after deconvolution, two separated oxidation peaks can be observed. The first peak at 265°C represents the oxidation of Fe^{2+} ions at B sites; this temperature has been determined previously [12] during the oxidation of spinels containing only Fe^{2+} ions on octahedral sites. Concerning region II, the oxidation proceeds through some distinguishable steps with a variation in intensity of the main peak. The large rise in intensity in the temperature range 350–550°C with the vanadium content corresponds to the oxidation of V^{3+} to V^{5+} ions. Indeed, the IR spectra of oxidized samples at various temperatures (Fig. 4) exhibit above 320°C (curves e and f) two absorption bands at 920 and 830 cm^{-1} assigned to the V^{5+} ions [21–23]. In addition, X-ray diffraction analysis revealed that above 450°C the oxidation takes place sequentially [24,25]. In the first stage of oxidation, the cation-deficient spinel is progressively converted into α-Fe_2O_3 (or a solid solution of V_2O_3 in Fe_2O_3 for high x values), whereas in the next stage of oxidation, above 600°C, the formation of iron(III) orthovanadate, $FeVO_4$, is also observed. The formation of this phase can be correlated with the oxidation of Fe^{2+} ions on A sites: in comparison with other mixed valency ferrites, it provides strong evidence for the presence of Fe ions in the divalent state [13].

As stated previously, in region I two peaks can be seen after deconvolution. The second peak centered at about 300°C represents the oxidation of vanadium ions

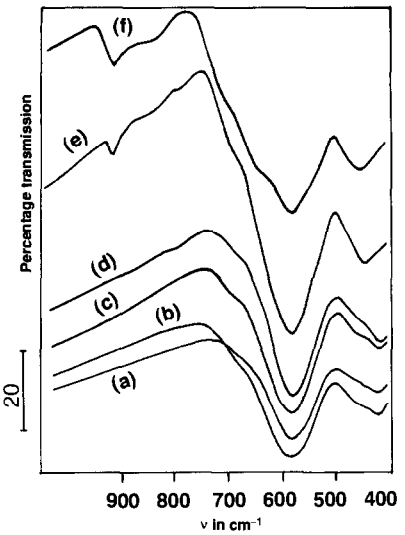

Fig. 4. V–O stretching frequencies for a sample with $x = 0.50$ oxidized at different temperatures. Each curve corresponds to an oxidation with the temperature increasing at a linear rate of 2.5°C min^{-1} and then stopping at the indicated temperature. (a) 250°C; (b) 285°C; (c) 270°C; (d) 315°C; (e) 322°C; (f) 350°C.

located at B sites. However, as the infrared spectra of samples oxidized below 320°C (Fig. 4, curves a, b, c and d) do not show the absorption bands at 920 and 830 cm^{-1} characteristic of V^{5+} ions, this peak can be attributed to vanadium oxidation, according to the charge equilibrium $V^{2+} + 0.5O_{ads} \rightarrow V^{3+} + 0.5O^{2-}$, on migration of V into an absorbed oxygen layer. In order to propose a cation distribution, a quantitative analysis of cations from the determination of oxidation peak areas has been investigated. For the determination of oxidation peak areas, where the peaks exhibit a tendency to overlap, the profile of each peak has been confirmed by DTG after selective oxidation in isothermal conditions. For example the profile of the peak attributed to the oxidation of V^{2+} ions has been defined after selective oxidation at 200°C for 24 h of Fe^{2+} ions at B sites (Fig. 5, curve b). A similar experimental procedure was adopted for the oxidation of V^{3+} ions on B sites after elimination by selective oxidation of Fe^{2+} and V^{2+} ions at 270°C for 24 h (Fig. 5, curve c). Consequently, the ascending portion of curve c represents only the oxidation of V^{3+} ions. These results suggest an ionic configuration for $Fe_{3-x}V_xO_4$ of the type

$$(Fe^{2+}_{\alpha} Fe^{3+}_{1-\alpha})_A (Fe^{2+}_{1-\alpha-\beta} Fe^{3+}_{1-x+\alpha+\beta} V^{2+}_{\beta} V^{3+}_{x-\beta})_B O^{2-}_4 \quad (6)$$

From the area of the Fe^{2+}_B and V^{2+}_B peaks, the α and β coefficients of configuration (6) can be determined and the evolution of these coefficients with vanadium content is shown in Fig. 6. Using these values, the coefficients for V^{3+} ions at B sites and Fe^{3+} ions at A sites may be obtained. Because of the weaker ionic bonding of

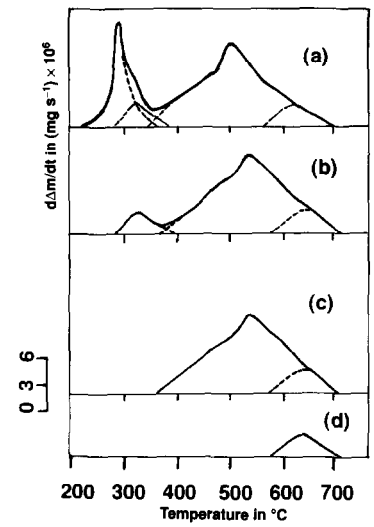

Fig. 5. DTG curves $d\Delta m/dt = f(T)$ showing the disappearance of the first (Fe_B^{2+}, curve b), second (V_B^{2+}, curve c), and third (V_B^{3+}, curve d) peaks after selective oxidation.

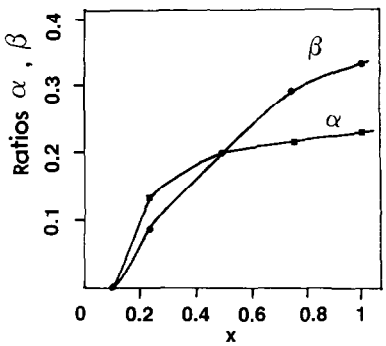

Fig. 6. Evolution of α and β ratios versus vanadium content.

and Fe^{3+} ions at A sites may be obtained. Because of the weaker ionic bonding of the B sites as compared with the stronger A-site covalent bonds, the fourth peak at about 600°C showing one defined oxidation state (Fig. 5, curve d) can be attributed to Fe^{2+} ions located at A sites. Indeed, from preliminary experiment, it has been established that this oxidation temperature closely corresponds to the temperature obtained for $FeCr_2O_4$, with Fe^{2+} ions at the A sites being the sole oxidizable cation [12].

There are also V^{2+} ions in this distribution, i.e. about 50% of all vanadium in Fe_2VO_4. Up to now, only one report has been made of the appearance of V^{2+} ions at the B sites [11]. The V^{2+}–O^{2-} distance of 0.2055 nm, shorter than the Fe^{2+}–O^{2-} distance of 0.2130 nm [26] appears convincingly to explain the difference in reactivity of these cations located on the B sites.

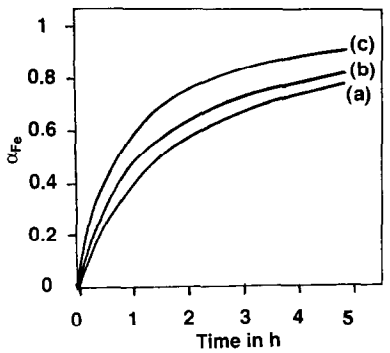

Fig. 7. Kinetic curves $\alpha_{Fe} = f(t)$ for the oxidation of octahedral Fe^{2+} ions of the pure magnetite. (a) 235°C; (b) 244°C; (c) 252°C.

We can calculate the lattice parameter for iron–vanadium spinels for a given cation distribution using the invariant character of the "cation–anion" distance established by Poix [27] from large numbers of crystal structure determinations. Fig. 1 shows a comparison of the experimental lattice parameters with values calculated from formula (6), taking the metal–oxygen distances from ref. 26. Neither our data, nor any of the data given in refs. 5, 14 and 15, fit the lattice constant data satisfactorily, particularly for x in the composition range 0.25–0.75. The basic assumption that the cation–anion distances in the A and B complexes are invariant, appears invalid here.

3.2. Mechanism of the oxidation of the V^{3+} ions

The possibility of every cation being oxidized independently enables us to study the oxidation kinetics of the various ions, particularly V_B^{3+}, that of Fe_B^{2+} having been previously investigated [19] and the concentration of V_B^{2+} being too low. In the case of the oxidation of sub-micron spinel ferrites, the reaction kinetics can be interpreted acceptably by considering diffusion, under variable working conditions, of the vacancies generated at the solid–gas interface. For example, in the case of the Fe_B^{2+} oxidation of pure magnetite (Fig. 7), the kinetic law can be described by the expression [28]

$$\alpha_{Fe} = \frac{1-6}{\pi^2} \sum_{n=1}^{\infty} (1/h^2) \exp(-n^2 k t) \tag{7}$$

where $k = \pi^2 \tilde{D}/a^2$, and $\tilde{D}$, a and α_{Fe} are the chemical diffusion coefficient, the mean grain radius and the degree of conversion, respectively. $\tilde{D}$ can be expressed by

$$\tilde{D} = D_0 \exp(-E/RT) \tag{8}$$

where D_0 is the frequency factor and E the activation energy for Fe_B^{2+} oxidation. In this case, $\tilde{D}$ is independent of vacancy content δ (Fig. 8).

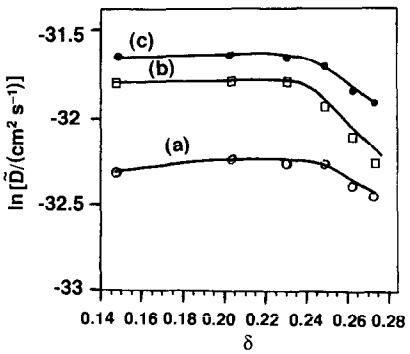

Fig. 8. Vacancy content dependence of the chemical diffusion coefficient for various oxidation temperatures of Fe_B^{2+} ions. (a) 235°C; (b) 244°C; (c) 252°C.

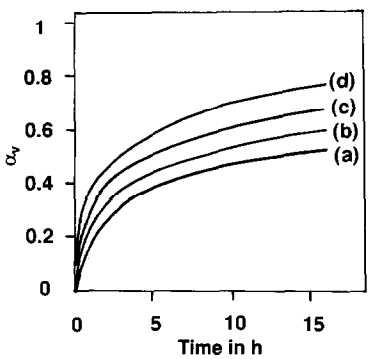

Fig. 9. Kinetic curves $\alpha_V = f(t)$ for oxidation of octahedral V^{3+} ions. (a) 370°C; (b) 380°C; (c) 390°C; (d) 400°C.

After total oxidation of the Fe_B^{2+} and V_B^{2+} ions at 270°C for 24 h, oxidation of the V_B^{3+} ions occurs; this can be studied at different isothermal temperatures. This reaction is characterized by an extremely rapid initial stage, declining regularily, and roughly obeying a parabolic law (Fig. 9). However, total analogy with the kinetic curves found for the Fe_B^{2+} oxidation is not observed because, at low temperatures, the reaction slows markedly after only a few hours and cannot be completed. This is assumed to be due to the decrease in the chemical diffusion coefficient with increasing vacancy content and is corroborated by studying the V_B^{3+} oxidation kinetics after total oxidation of the Fe_B^{2+} and V_B^{2+} ions, i.e. when a large number of vacancies is present in the crystal lattice. For example, in the case of a substituted magnetite with $x = 0.50$, the oxidation of V_B^{3+} ions is carried out from the defect spinel

$$(Fe^{2+}_{0.182}Fe^{3+}_{0.818})_A(Fe^{3+}_{1.272}V^{3+}_{0.454}\square_{0.272})_B O_4^{2-} \quad (9)$$

where □ denotes the cation vacancies.

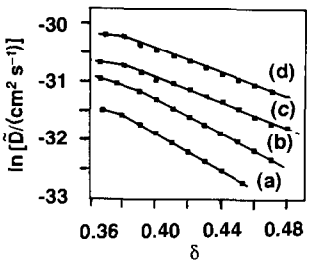

Fig. 10. Vacancy content dependence of the chemical diffusion coefficient for various oxidation temperatures of V_B^{3+} ions. (a) 370°C; (b) 380°C; (c) 390°C; (d) 400°C.

Moreover, the oxidation reaction

$$\tfrac{5}{8}Fe_{Fe_A(III)} + V_{Fe_B(II)} + \tfrac{1}{2}O_2 \rightarrow$$
$$V''_{Fe_A(III)} + O_0 + \tfrac{1}{2}V'''_{Fe_B(III)} + \tfrac{1}{2}V''_{Fe_B(II)} + \tfrac{5}{8}Fe_{Fe_B(III)} \quad (10)$$

generates an important amount of additional vacancies.

The decrease in the chemical diffusion coefficient with increasing vacancy concentration (Fig. 10) can be partly explained by introducing vacancy association and/or interaction between cation vacancies and electron holes. Thus, the chemical diffusion coefficient is given by the expression [13]

$$\tilde{D} = K_0 \exp(-E_a/RT) \exp(-b\delta) \quad (11)$$

where K_0 and b are constants and E_a is the activation energy for the oxidation of V_B^{3+} ions.

Under these conditions, for an isothermal reaction, the vacancy content δ, and consequently $\tilde{D}$, depend on the reaction time only. A diffusion-controlled reaction involving a composition gradient through spherical particles, can be described by the Fick equation

$$\frac{\partial C}{\partial t} = \tilde{D}(t)\frac{1}{r^2}\frac{\partial}{\partial r}\left(r^2\frac{\partial C}{\partial r}\right) \quad (12)$$

With a change in variable, $u = rC$, and by introducing the variable Z such that $z = \int_0^t \tilde{D}(t)\,dt$, Eq. (12) can be written

$$\frac{\partial u}{\tilde{D}(t)\partial t} = \frac{\partial^2 u}{\partial r^2} \quad (13)$$

which leads to

$$\alpha_V = 1 - 6/\pi^2 \sum_{n=1}^{\infty}\frac{1}{n^2}\exp\left(-n^2\frac{\pi^2}{a^2}\int_0^t \tilde{D}(t)\,dt\right) \quad (14)$$

From the variation of $\ln \tilde{D}$ versus $1/T$ for various α_V values, an activation energy of 180 kJ mol^{-1} is obtained for $x = 0.50$. This value is lower than that relative to the oxidation of Mo^{3+} ions in molybdenum spinels with the same substitution

content ($E = 226$ kJ mol^{-1}). Moreover, the constant b depends on the temperature and obeys the equation [29]

$$b = b_0 \exp(-E_{diss}/RT) \tag{15}$$

According to this equation, E_{diss} is defined as the dissociation energy of vacancies and electron holes which leads to an exponent of $P(O_2)$ greater than the value calculated considering a total association [30]. A value of 89 kJ mol^{-1} was obtained, whereas for Mo-substituted magnetites, the constant b was temperature independent [29].

If we consider an association reaction of the type $V''_{M_{II}} + h^{\cdot} \rightleftharpoons V'_{M_{II}}$, the mass action law gives

$$\frac{[V''_{M_{II}}][h^{\cdot}]}{[V_{M_{II}}]} = Cte = \exp\left(\frac{\Delta G_0}{kT}\right) = K \exp\left(\frac{\Delta H_0}{kT}\right) \tag{16}$$

where ΔG_0 is the free enthalpy of the association reaction. This reaction being exothermic, ΔH_0 is negative and, in neglecting the entropy term, the concentration in free defects increases with temperature.

4. Conclusions

These results show that vanadium-substituted magnetites $Fe_{3-x}V_xO_4$ with $0 < x < 1$ prepared at relatively low temperature by a ceramic route and having a crystallite size close to 0.3 μm, are highly reactive with oxygen. Consequently, they could be partly oxidized below 500°C to form cation-deficient spinels with a larger vacancy content than in γ-Fe_2O_3. The DTG curves exhibit four stages in the oxidation process, the oxidation temperatures of which are related to the distribution of Fe^{2+}, V^{2+} and V^{3+} ions at the B sites and of Fe^{2+} ions at the A sites. The temperatures of each peak, being associated with the oxidation process provide the following trend in stability towards oxidation: $(Fe^{2+}-O^{2-})_B < (V^{2+}-O^{2-})_B < (V^{3+}-O^{2-})_B < (Fe^{2+}-O^{2-})_A$.

A quantitative analysis on the cation distribution from the determination of oxidation peak areas based on this discrepancy of reactivity enables the calculation of the α and β coefficients relative to the ionic configuration

$$(Fe^{2+}_{\alpha} Fe^{3+}_{1-\alpha})_A (Fe^{2+}_{1-\alpha-\beta} Fe^{3+}_{1-x+\alpha+\beta} V^{2+}_{\beta} V^{3+}_{x-\beta})_B O^{2-}_4$$

The oxidation kinetics under isothermal conditions of V^{3+} ions after selective oxidation of Fe^{2+}_B and V^{2+}_B ions has established that the kinetics, as for Mo^{3+} ions in molybdenum spinels, is controlled by a diffusion process involving a composition gradient through particles of a non-stoichiometric spinel, with the diffusion coefficient being dependent on the vacancy content. It is believed that the association phenomena are partly responsible for the decrease in the chemical diffusion coefficient and that this, in turn, determines its effect with temperature.

In this respect, we consider that, in addition of the formation of a high concentration in vacancies, the lattice parameter sharply decreases with oxidation

content. Because of a concentration gradient, the oxidation produces inhomogeneous grains when the outside is more oxidized than the interior [31] and generates stresses in the ferrite particles. These stresses can also be responsible for the variation in the chemical diffusion coefficient.

References

[1] D.B. Rogers, R.J. Arnott, A. Wold and J.B. Goodenough, J. Phys. Chem. Solids, 24 (1963) 347.
[2] M.J. Rossiter, J. Phys. Chem. Solids, 26 (1965) 775.
[3] S.K. Baneejee, W. O'Reilly, T.C. Gibb and N.N. Greenwood, J. Phys. Chem. Solids, 28 (1967) 1323.
[4] M.P. Gupta and H.B. Mathur, J. Phys. C. Solid State Phys., 8 (1975) 370.
[5] M. Wakihara, Y. Shimizu and T. Katsura, J. Solid State Chem., 3 (1971) 478.
[6] M. Abe, Kawachi and S. Nomura, J. Solid State Chem., 10 (1974) 351.
[7] B.N. Varskoi, A.N. Il'ina and N.N. Gogareva, Russ, J. Phys. Chem., 40 (1966) 447.
[8] J.D. Lee and D. Schroeer, J. Phys. Chem. Solids, 37 (1967) 739.
[9] E. Riedel, A. Ostermann and J. Kahler, Z. Naturforsch. Teil B, 44 (1989) 869.
[10] K. Mizushima, M. Tanaka, A. Asai, S. Iida and J.B. Goodenough, J. Phys. Chem. Solids, 40 (1979) 1129.
[11] J. Bernier and P. Poix, Ann. Chim. Fr., 2 (1967) 1981.
[12] B. Gillot, F. Jemmali, F. Chassagneux, C. Salvaing and A. Rousset, J. Solid State Chem., 45 (1982) 317.
[13] B. Domenichini, B. Gillot, P. Tailhades, L. Bouet and A. Rousset, Solid State Ionics, 58 (1992) 61.
[14] M. Lensen, Ann. Chim., 4 (1959) 891.
[15] B. Gros, Bull. Soc. Chim. Fr., 9–10 (1976) 1381.
[16] M. Ishii and M. Nakahira, Solid State Commun., 11 (1972) 209.
[17] A.V. Serebryakova, N.A. Vatolin, P.I. Volkova, T.V. Sapozhnikova, A.A. Ryzhov and S.B. Shibaeva, Izv. Akad. Nauk SSSR, Neorg. Mater., 11 (1975) 1440.
[18] E. Riedel and N. Pleil, Z. Naturforsch., 35 (1980) 1261.
[19] B. Gillot, A. Rousset and G. Dupre, J. Solid State Chem., 25 (1978) 263.
[20] M. Laarj, I. Pignone, M. El Guendouzi, P. Tailhades, A Rousset and B. Gillot, Thermochim. Acta, 152 (1989) 187.
[21] L.D. Frederickson, Jr, Anal. Chem., 35 (1963) 818.
[22] E.J. Baran and P.J. Aymonino, Z. Anorg. Allg. Chem., 365 (1969) 211.
[23] G. Fabbri and P. Baraldi, Anal. Chem., 44 (1972) 1325.
[24] A.A. Ryshov, N.A. Vatolin, P.I. Volkova and V.F. Balakirev, Kinet. Catal., 12 (1971) 934.
[25] P.P. Stander and C.P.J. van Vuuren, Thermochim. Acta, 157 (1990) 347.
[26] P. Poix, C.R. Acad. Sci., Paris, 268 (1969) 1139.
[27] P. Poix, Séminaire de Chimie Etat Solide, Liaisons interatomiques et propriétés physiques des composés Minéraux, Paris, Seides, 1967.
[28] B. Gillot, D. Delafosse and P. Barret, Mater. Res. Bull., 8 (1973) 1431.
[29] B. Domenichini and B. Gillot, Solid State Ionics, 57 (1992) 11.
[30] B. Gillot, Mat. Res. Bull., 15 (1980) 31.
[31] T. Nishitani, Rock Mag. Paleogeophys., 6 (1979) 128.